Front. Phys. 12(5), 120509 (2017)
DOI 10.1007/s11467-017-0687-5

RESEARCH ARTICLE

Dynamical phase transitions in a two-species bosonic Josephson junction

Jing Tian†, Jun Liu, Hai-Bo Qiu, Xiao-Qiang Xi

School of Science, Xi'an University of Posts and Telecommunications, Xi'an 710121, China
Corresponding author. E-mail: †tianj2005@gmail.com
Received January 25, 2017; accepted April 19, 2017

We investigate dynamical phase transitions that are induced by interspecies interaction in a two-species bosonic Josephson junctions (BJJ), based on semi-classical theory. In zero-phase mode, similar to the case of a single-species BJJ, we observe the well-known dynamical phase transition from Josephson oscillation to self-trapping, which can be induced by both enhanced repulsive and attractive interspecies interactions. In π phase mode, dynamical phase transitions are even more interesting and counter-intuitive. We characterize a dynamical phase transition with the merging of two separate phase space domains into one, which is induced by increasing repulsive interspecies interaction. On the other hand, we find that by increasing attractive interspecies interaction, a phase separation of two formally overlapped phase space domains will occur. At last, we reveal that these intriguing dynamical phase transitions are caused by different kinds of bifurcations.

Keywords dynamical phase transition, bosonic Josephson junction

PACS numbers 05.45.Mt, 64.60.-i, 03.75.Mn, 45.20.Jj

1 Introduction

The investigation of Bose–Einstein condensates (BECs) has led to a wide spread interest in nonlinear quantum dynamics during the past few decades [1–5]. In the context of BECs, the nonlinearity stems from atomic collisions. This leads to Gross–Pitaevskii type of nonlinear Schrödinger equations, which is widely used for the study of BECs [3]. Due to the atomic field nonlinearity, several interesting nonlinear phenomena have been revealed in BECs, such as soliton [6], vortex [7], self-trapping [8], and measure synchronization [9].

Bosonic Josephson junction (BJJ) is one of the simplest set-ups in exploring nonlinear quantum dynamics for BECs, which can be created by trapping BECs in a double well potential. Smerzi *et al.* found that the system of a single species BECs trapped in a double well potential, so called a single species BJJ, can be mapped into a classical inverted pendulum system. They predicted the self-trapping phenomenon and discussed the dynamical phase transition behavior from Josephson oscillation to self-trapping with the phase-plane portrait [8]. Later on, self-trapping had been investigated extensively, both theoretically and experimentally [10–18].

The theoretical interests have been extended to a two-species BJJ [19]; Josephson oscillations in a two-species BJJ have been addressed in a number of studies [20–22]. The self-trapping has also been discussed [23], and many novel tunneling effects have been found, such as the symmetry restoring phase [24] and mixed Rabi–Josephson oscillations [25].

The nonlinear dynamics in a two-species BJJ are much more complex compared with the case of a single species BJJ because there are two different kinds of nonlinear terms appearing, namely, the intraspecies interaction and interspecies interaction. In our previous works [9, 26], we exploited measure synchronization induced by enhanced interspecies interaction for a two-species BJJ based on phase space analysis. Here we generalize our discussions to investigate various dynamical phase transitions induced by interspecies interactions.

This paper is organized as follows. A brief description of a two-species BJJ model is given in Section 2. The stationary solutions of semiclassical theory for the two-species BJJ model is present in Section 3. In Section 4, we discuss different dynamical phase transitions induced by enhanced interspecies interactions. Section 5 reveals the dynamical mechanism behind these dynamical phase transitions. Conclusions are given in Section 6.

2 The model

A two-species BJJ can be experimentally realized by trapping a binary mixture of BECs in a symmetric double well potential. By assuming that the interaction among the atoms is sufficiently weak, with the well-known two-mode approximation [8, 27, 28], the Hamiltonian in the second quantization reads

$$\begin{aligned}\hat{H} = &\frac{u_a}{2N_a}[(\hat{a}_L^\dagger\hat{a}_L)^2+(\hat{a}_R^\dagger\hat{a}_R)^2]+\frac{u_b}{2N_b}[(\hat{b}_L^\dagger\hat{b}_L)^2+(\hat{b}_R^\dagger\hat{b}_R)^2]\\ &-\frac{v_a}{2}(\hat{a}_L^\dagger\hat{a}_R+\hat{a}_R^\dagger\hat{a}_L)-\frac{v_b}{2}(\hat{b}_L^\dagger\hat{b}_R+\hat{b}_R^\dagger\hat{b}_L)\\ &+\frac{u_{ab}}{\sqrt{N_aN_b}}(\hat{a}_L^\dagger\hat{a}_L\hat{b}_L^\dagger\hat{b}_L+\hat{a}_R^\dagger\hat{a}_R\hat{b}_R^\dagger\hat{b}_R),\end{aligned} \tag{1}$$

where $\hat{a}_{L(R)}^\dagger$ ($\hat{a}_{L(R)}$) and $\hat{b}_{L(R)}^\dagger$ ($\hat{b}_{L(R)}$) are the creation (annihilation) operators for the localized modes in the left (L) or right (R) well of different species (a or b), respectively. N_a and N_b stand for the particle numbers of species a and b. $u_\sigma = (4\pi\hbar a_\sigma N_\sigma/m_\sigma)\int|\varphi_\sigma|^4\mathrm{d}r$, $u_{ab} = 2\pi\hbar a_{ab}\sqrt{N_aN_b}(\frac{1}{m_a}+\frac{1}{m_b})\int|\varphi_a|^2|\varphi_b|^2\,\mathrm{d}r$ denote the effective interaction of atomic collisions between the same kind of species, and between different species, respectively, with $\sigma = a, b$ as the indication of species. The interactions can be either repulsive or attractive, depending on the sign of u. Either u_a, u_b and u_{ab} can be tuned by Feshbach resonance technique, as demonstrated by experiments in the mixture of ^{87}Rb and ^{85}Rb [29]. $v_\sigma = \int[(\hbar^2/(2m_\sigma))\nabla\varphi_L\nabla\varphi_R + V(r)\varphi_L\varphi_R]\mathrm{d}r$ is the effective Rabi frequency describing the coupling between the two wells.

Under the semi-classical limit [8, 27, 28], the dynamics of the system can be described by a classical Hamiltonian $H = \langle\Psi_{GP}|\hat{H}|\Psi_{GP}\rangle/N$, in which $|\Psi_{GP}\rangle = \frac{1}{\sqrt{N_a}}(\alpha_L\hat{a}_L^\dagger + \alpha_R\hat{a}_R^\dagger)^{N_a}|0,0\rangle\bigotimes\frac{1}{\sqrt{N_b}}(\beta_L\hat{b}_L^\dagger+\beta_R\hat{b}_R^\dagger)^{N_b}|0,0\rangle$ is the collective state of the N-particle system with $N = N_a + N_b$. Here, $\alpha_j = |\alpha_j|e^{i\theta_{aj}}$ and $\beta_j = |\beta_j|e^{i\theta_{bj}}$ ($j = L$ or R) are four c numbers which correspond to the probability amplitudes of the two different species of atoms in the two wells. The conservation of particle numbers of each species requires: $|\alpha_L|^2 + |\alpha_R|^2 = 1$, $|\beta_L|^2 + |\beta_R|^2 = 1$.

By introducing the relative population difference: $S_a = |\alpha_L|^2 - |\alpha_R|^2$, $S_b = |\beta_L|^2 - |\beta_R|^2$, and the relative phase difference $\theta_\sigma = \theta_{\sigma L} - \theta_{\sigma R}$, we obtain the mean-field Hamiltonian [19],

$$H_{tot} = H_a + H_b + H_I. \tag{2}$$

It is composed of Hamiltonian H_σ ($\sigma = a, b$)

$$H_\sigma = \frac{u_\sigma}{2}S_\sigma^2 - v_\sigma\sqrt{1-S_\sigma^2}\cos\theta_\sigma, \tag{3}$$

and the coupling term

$$H_I = u_{ab}S_aS_b. \tag{4}$$

H_σ is well known as the mean field Hamiltonian for a single-species BJJ [8, 27]; H_I is the coupling term. Thus, a two-species BJJ is similar to two coupled single-species BJJs. It is clear that the coupling exists due to the presence of the interspecies interaction u_{ab}.

The equations of motion can be derived by computing: with $\dot{\theta_\sigma} = \frac{\partial H}{\partial S_\sigma}$, $\dot{S_\sigma} = -\frac{\partial H}{\partial\theta_\sigma}$, we obtain

$$\dot{\theta_a} = u_aS_a + \frac{v_aS_a}{\sqrt{1-S_a^2}}\cos\theta_a + u_{ab}S_b, \tag{5}$$

$$\dot{S_a} = -v_a\sqrt{1-S_a^2}\sin\theta_a, \tag{6}$$

$$\dot{\theta_b} = u_bS_b + \frac{v_bS_b}{\sqrt{1-S_b^2}}\cos\theta_b + u_{ab}S_a, \tag{7}$$

$$\dot{S_b} = -v_b\sqrt{1-S_b^2}\sin\theta_b. \tag{8}$$

The tunneling dynamics of a two-species BJJ can be described with Eqs. (5)–(8). Here, the standard fourth-order Runge–Kutta method is employed to obtain numerical solutions. Following our previous methodology [26], the dynamics are presented by projecting the state of the full system onto the individual phase spaces, i.e., we study the trajectories $(S_a(t), \theta_a(t))$ in the phase plane (S_a, θ_a) and the trajectories $(S_b(t), \theta_b(t))$ in the phase plane (S_b, θ_b).

The tunneling dynamics for a single-species BJJ have been extensively studied [8, 13–18, 27, 28], and the studies of H_σ based on the semi-classical theory have shown that there are two distinct dynamic regimes in the phase-plane portrait [8, 18, 27]: the Josephson oscillation regime and the self-trapping regime with a strong nonlinearity ($u/v > 1$). For simplicity, 0-phase stands for the Josephson oscillation, in which θ_σ oscillates around $\theta_\sigma = 0$, and π-phase stands for the self-trapping regime, in which θ_σ oscillates around $\theta_\sigma = \pi$. To show the coupled dynamical behavior of H_σ, we then categorize the initial configurations of a two-species BJJ into two broad categories: i) 0-phase mode, ii) π-phase mode.

3 Stationary solutions: Fixed points

Let us first discuss the fixed point solutions of the classical Hamiltonian for a two-species BJJ. The fixed points can be derived from Eqs. (5)–(8), and we have

$$S_a = -\frac{1}{u_{ab}}\left(u + \frac{v\cdot\cos\theta_b}{\sqrt{1-S_b^2}}\right)S_b, \tag{9}$$

$$S_b = -\frac{1}{u_{ab}}\left(u + \frac{v\cdot\cos\theta_a}{\sqrt{1-S_a^2}}\right)S_a, \tag{10}$$

here $\theta_i = 0$ or $\theta_i = \pi$, with $i = a$ or b.

For $S_a = S_b$, the fixed point solutions are

$$S_j = \pm\sqrt{1 - \frac{v^2}{(u+u_{ab})^2}}, \tag{11}$$

here $-1 \le S_j \le 1$, with $j = a$ or b.

For $S_a = -S_b$, the fixed point solutions are

$$S_j = \pm\sqrt{1 - \frac{v^2}{(u-u_{ab})^2}}, \tag{12}$$

here $-1 \le S_j \le 1$, with $j = a$, or b.

For $|S_a| \neq |S_b|$, the analytic solutions cannot be obtained, and we need to solve it numerically.

One can divide the above fixed point solutions into four different categories: i) symmetrical ("S"): $S_a = S_b$; ii) anti-symmetrical ("An"): $S_a = -S_b$; iii) isotropic ("I"): $S_a = S_b = 0$, for the trivial case; iv) asymmetrical ("As"): $|S_a| \neq |S_b|$. We can also divide the fixed point solutions based on the value of θ_i being chosen, with $\theta_i = 0$ denoting the 0-phase mode, and $\theta_i = \pi$ denoting the π-phase mode. There are four different phase modes under this classification, including $(\theta_a, \theta_b) = \{(0,0), (\pi,\pi), (\pi,0), (0,\pi)\}$.

Now let us discuss the number changes of the fixed points in parameter space and their stability. In order to analyze stability of fixed points, the infinitesimal variables δ_a and δ_b are introduced by considering $S_a = S_a^0 + \delta_a$, $S_b = S_b^0 + \delta_b$, with S_a^0 and S_b^0 satisfying Eqs. (9)–(10). From Eqs. (5)–(8), the linearized equations of motion for $(\theta_a, \theta_b) = (0,0)$ are derived,

$$\begin{bmatrix} \delta_a'' \\ \delta_b'' \end{bmatrix} = -\Omega \begin{bmatrix} \delta_a \\ \delta_b \end{bmatrix}. \tag{13}$$

Here,

$$\Omega = \begin{bmatrix} \omega_{11} & \omega_{12} \\ \omega_{21} & \omega_{22} \end{bmatrix}, \tag{14}$$

$\omega_{11} = v^2 + vu\sqrt{1-(S_a^0)^2} + (uS_a^0 + u_{ab}S_b^0)^2$, $\omega_{12} = vu_{ab}\sqrt{1-(S_a^0)^2}$, $\omega_{21} = vu_{ab}\sqrt{1-(S_b^0)^2}$, $\omega_{22} = v^2 + vu\sqrt{1-(S_b^0)^2} + (uS_b^0 + u_{ab}S_a^0)^2$.

The eigenvalues of Ω correspond to the square of eigenfrequencies of the linearized dynamical system, which are

$$\lambda_\pm^2 = v^2 + \frac{(C_1^2 + C_2^2) + vu(D_1 + D_2)}{2} \pm \frac{1}{2}\sqrt{\left[(C_1^2 - C_2^2) + vu(D_1 - D_2)\right]^2 + 4v^2u_{ab}^2 D_1 D_2}, \tag{15}$$

with $C_1 = uS_a^0 + u_{ab}S_b^0$, $C_2 = uS_b^0 + u_{ab}S_a^0$, $D_1 = \sqrt{1-(S_a^0)^2}$, $D_2 = \sqrt{1-(S_b^0)^2}$.

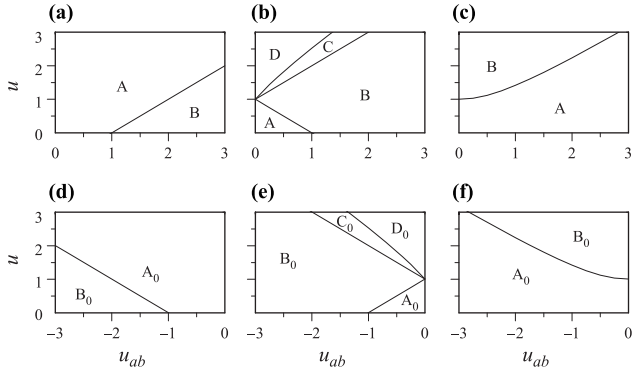

Fig. 1 Multiple existence and stability diagrams of the fixed points in the (u_{ab}, u) phase plane for different phase modes. **(a, b)** and **(c)** are for $(0,0)$, (π,π), and $(0,\pi)$ phase modes with $u_{ab} > 0$, respectively. **(d, e)** and **(f)** are for $(0,0)$, (π,π), and $(0,\pi)$ phase modes with $u_{ab} < 0$, respectively. A-D and A_0-D_0 stand for the different kinds of dynamical regions for the fixed points.

The fixed points are dynamically stable as long as the corresponding eigenfrequencies λ_+ and λ_- are both real. In a similar way, we can derive the stability analysis results for fixed points in $(\theta_a, \theta_b) = (\pi,\pi)$, $(\pi,0)$, and $(0,\pi)$ phase modes.

The stability analysis results for the fixed points are plotted in Fig. 1, where Figs. 1(a) and (d) are for $(\theta_a, \theta_b) = (0,0)$ phase mode. Figures 1(b) and (e) are for $(\theta_a, \theta_b) = (\pi,\pi)$ phase mode. Figures 1(c) and (f) are for $(\theta_a, \theta_b) = (0,\pi)$ phase mode. The result for $(\theta_a, \theta_b) = (\pi,0)$ mode is the same as that for $(\theta_a, \theta_b) = (0,\pi)$ phase mode because we are considering two identical systems, and the two systems a and b are commutable.

For repulsive interspecies interactions ($u_{ab} > 0$), here A stands for the region with only 1 stable "I". B stands for region with 1 unstable "I" and 2 stable "An". C for the region with 1 unstable "I", 2 stable "S", and 2 unstable "An". D for region with 1 unstable "I", 2 stable "S", 2 stable "An", and 4 unstable "As". For attractive interspecies interactions ($u_{ab} < 0$), there is 1 stable "I" in the region A_0; there are 1 unstable "I" and 2 stable "S" in the region B_0; 1 unstable "I", 2 stable "An", and 2 unstable "S" in the region C_0; there are 1 unstable "I", 2 stable "An", 2 stable "S", and 4 unstable "As" in the region D_0.

4 Dynamical phase transitions for 0- and π-phase mode

As shown in our previous works [9, 26], the phase-space domains can be used to illustrate global dynamical changes of the system. Using the same methodology, we investigate dynamical phase transitions in the two-

species BJJ system for $(\theta_a, \theta_b) = (0, 0)$ and $(\theta_a, \theta_b) = (\pi, \pi)$ phase modes.

4.1 0-phase mode

Figures 2 shows the evolution process with increasing repulsive interspecies interactions, with the initial configuration (S_a, S_b, θ_a, θ_b) being (0.2, 0.4, 0, 0). We draw orbits on the (S_σ, θ_σ) phase plane of the two subsystems, with $\sigma = a$, and b. For $u_{ab} = 0$, as shown in Fig. 2(a), these initial conditions correspond to two different quasiperiodic orbits, which cover closed curves in green and black. For $u_{ab} > 0$, the two closed curves are replaced with two smooth quasi-periodic trajectories wandering in two distinctive phase-space domains, being ring shaped. As u_{ab} increases, the two phase-space domains first evolve such that the external border of the inner domain approaches the internal border of the outer domain, and the two approach each other until $u_{ab} = 0.0086$, at which point the two approaching boundaries are almost in contact with each other [Fig. 2(b)]. Then, a sudden change occurs when u_{ab} increases further, as shown in Fig. 2(c). The two formally well-separated phase-space domains merge and cover the phase-space domains with an identical invariant measure [30]. This dynamical phase transition of the two phase-space domains marks the transition to measure synchronization [26]. For $u_{ab} = 2.1$ [Fig. 2(d)], the system keeps in MS states. However, by continually increasing interspecies interaction up to $u_{ab} = 2.2$ [Fig. 2(e)], another dynamical phase transition of the system is characterized, with phase-space domains shifting into two orbits which lie symmetric with respect to $S_\sigma = 0$ ($\sigma = a, b$). As shown in Fig. 2(f), when $u_{ab} = 2.3$, the evolution orbits of the system indeed lie symmetric with respect to $S_\sigma = 0$, ($\sigma = a, b$). The new configuration correspond to a novel symmetry breaking state,

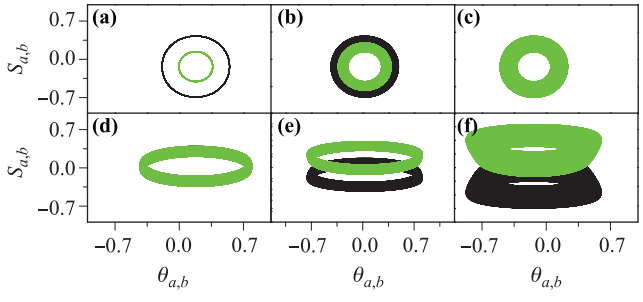

Fig. 2 Phase-space domains of the two species in the 0-phase mode for $u_{ab} > 0$. The two species are represented by green and black. Initial configuration (S_a, S_b, θ_a, θ_b) set to be (0.2, 0.4, 0, 0). **(a)** $u_{ab} = 0$, **(b)** $u_{ab} = 0.0086$, **(c)** $u_{ab} = 0.0087$; MS is achieved. **(d)** $u_{ab} = 2.1$, **(e)** $u_{ab} = 2.2$, Nonlocal MS is achieved. **(f)** $u_{ab} = 2.3$.

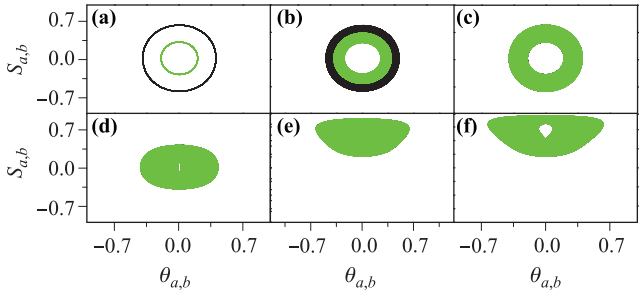

Fig. 3 Phase-space domains of the two species in the 0-phase mode for $u_{ab} < 0$. The two species are represented by green and black. Initial configuration (S_a, S_b, θ_a, θ_b) set to be (0.2, 0.4, 0, 0). **(a)** $u_{ab} = 0$, **(b)** $u_{ab} = -0.0737$, **(c)** $u_{ab} = -0.0738$, MS is achieved. **(d)** $u_{ab} = -1.7$, **(e)** $u_{ab} = -2.2$, **(f)** $u_{ab} = -2.6$.

which is self-trapped, with a non-zero averaging population imbalance in the 0-phase mode. This dynamical change marks the dynamical phase transition from Josephson oscillation to self-trapping.

Figures 3(a)–(f) show the evolution process with increasing strength of attractive interspecies interactions in the 0-phase mode, with initial configuration (S_a, S_b, θ_a, θ_b) being (0.2, 0.4, 0, 0). Start with Fig. 3(a), where we plot the orbits for each species with $u_{ab} = 0$. As u_{ab} decreases, at first, we characterize MS transition occurring at $u_{ab} = -0.0738$ [see Fig. 3(c)]. However, with interspecies interaction strength increasing up to $u_{ab} = -2.2$, as shown in the Fig. 3(e), another dynamical phase transition is characterized. Similar to the case of repulsive interspecies interactions in the 0-phase mode, this second dynamical change also marks the dynamical phase transition from Josephson oscillation to self-trapping, albeit being localized in the phase space picture compared with the nonlocalized case above.

Summarizing the above results, with increasing repulsive interspecies interaction, besides MS, we find that another dynamical phase transition happens for the 0-phase mode at $u_{ab} = 2.2$. It corresponds to a phase transition from Josephson oscillation to self-trapped states, which we also called nonlocal MS transition [31]. By increasing attractive interspecies interaction strength, besides the usual MS transition, we find that the second dynamical phase transition occurs at $u_{ab} = -2.2$. It also leads to self-trapped states, nonetheless, to be localized.

4.2 π-phase mode

In the π phase mode, the dynamical changes are much more complicated. Figure 4 shows the case of the evolution scenario for repulsive interspecies interactions. The initial configurations (S_a, S_b, θ_a, θ_b) are set to be (0.2, 0.4, π, π). With $u_{ab} = 0$, two closed curves are shown [see

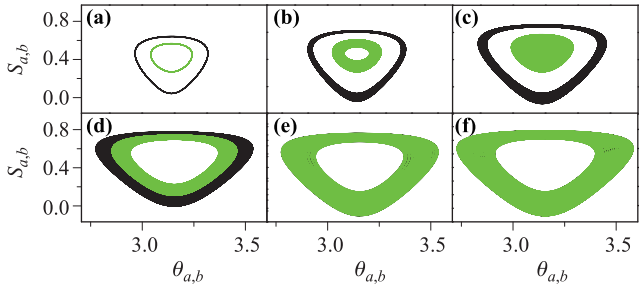

Fig. 4 Phase-space domains of the two species in the π-phase mode for $u_{ab} > 0$. The two species are represented by green and black. Initial configuration (S_a, S_b, θ_a, θ_b) set to be (0.2, 0.4, π, π). **(a)** $u_{ab} = 0$, **(b)** $u_{ab} = 0.03$, **(c)** $u_{ab} = 0.0737$, **(d)** $u_{ab} = 0.1621$, **(e)** $u_{ab} = 0.1622$, MS is achieved. **(f)** $u_{ab} = 0.3$.

Fig. 4(a)]. By increasing u_{ab}, the two closed curves are replaced by two distinctive phase-space domains, with a tendency that the outer boundary of the inner domain and inner boundary of the outer domain come close to each other [see Figs. 4(b)–(d)]. However, with interspecies interaction increasing up to $u_{ab} = 0.1622$, a phase transition of the system happens [see Fig. 4(e)] and the dynamical phase evolution of the system shifts from the separated phase-space domains into overlapped phase-space domains. The two phase-space domains cover the same acreage, and the system reaches the measure synchronization. As we keep increasing u_{ab}, the system remains in MS [see Fig. 4(f) for $u_{ab} = 0.3$].

Figure 5 shows the case of the evolution scenario for attractive interspecies interactions in the π phase mode, with initial configuration (S_a, S_b, θ_a, θ_b) being (0.2, 0.4, π, π). There we find the usual MS scenario in the first place; as $|u_{ab}|$ increases, the two separate phase-space regions approach each other until u_{ab} reaches the critical strength $u_c = -0.0123$ [Fig. 5(c)]. However, by further increasing the interspecies interaction strength, we find MS breakout with the emergence of chaos after u_{ab} reaches -0.0351; then, as $|u_{ab}|$ further increases, a new dynamical phase transition appears after the system crosses this chaotic regime. Now the two phase-space domains suddenly separate from each other, with the original inner domain on top of the other. See Fig. 5(e) with $u_{ab} = -0.18$. This corresponds to an interesting physical change; two species initially trapped in the same well are separated and are trapped in different wells when the attractive interspecies interaction strength exceeds a critical value. After this sudden change, by further increasing u_{ab} up to -0.186 [Fig. 5(f)], the nonlocal MS will be reached, with the phase-space domains of each species lying symmetric with respect to $S_\sigma = 0$ and covering the same acreage in phase space.

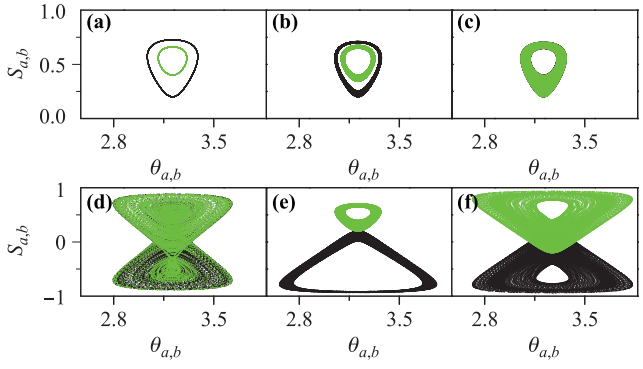

Fig. 5 Phase-space domains of the two species in the π-phase mode for $u_{ab} < 0$. The two species are represented by green and black. Initial configuration (S_a, S_b, θ_a, θ_b) set to be (0.2, 0.4, π, π). **(a)** $u_{ab} = 0$. **(b)** $u_{ab} = -0.01$. **(c)** $u_{ab} = -0.0123$; MS is achieved. **(d)** $u_{ab} = -0.105$. **(e)** $u_{ab} = -0.180$. **(f)** $u_{ab} = -0.186$; Nonlocal MS is achieved.

Summarizing the above results, for the π-phase mode with repulsive interspecies interaction, there is only one dynamical phase transition being characterized, the MS transition at $u_{ab} = 0.1622$. However, for the π-phase mode with attractive interspecies interaction, we find that three dynamical phase transitions exist; there are two MS transitions and another counter-intuitive phase separation.

4.3 Nonlocalized π-phase mode

For the π-phase mode, there exists a nonlocalized π-phase mode [26]. As such, with initial conditions (S_a, θ_a, S_b, θ_b) = (-0.2, π, 0.4, π), we have found new coherent evolutions. At $u_{ab} = 0$, these initial conditions also correspond to two closed curves, but with one curve on top of the other [Fig. 6(a)].

As the strength of repulsive interspecies interaction increases, the phase-space domains of the two species

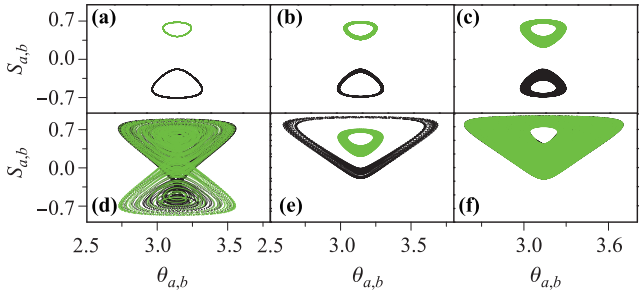

Fig. 6 Phase-space domains of the two species in the nonlocalized π-phase mode for $u_{ab} > 0$. The two species are represented by green and black. Initial configuration (S_a, S_b, θ_a, θ_b) set to be (-0.2, 0.4, π, π). **(a)** $u_{ab} = 0$. **(b)** $u_{ab} = 0.01$. **(c)** $u_{ab} = 0.0123$; nonlocal MS is achieved. **(d)** $u_{ab} = 0.105$. **(e)** $u_{ab} = 0.18$. **(f)** u_{ab}=0.186; MS is achieved.

become more comparable in acreage until u_{ab} reaches a critical value $u_c = 0.0123$; a sudden change then occurs, as shown in Fig. 6(c), and the two phase-space domains now have the same acreage. The nonlocal MS is being reached. However, by further increasing the interspecies interaction strength, we find nonlocal MS breakout with the emergence of chaos after u_{ab} reaches 0.0351; then, as u_{ab} further increases, a new dynamical phase transition appears after the system crosses this chaotic regime. Now the two phase-space domains suddenly move to the same side of the S_σ axis, being localized. See Fig. 6(e) with $u_{ab} = 0.18$. This corresponds to an interesting physical change; two species initially trapped in different wells are separated and trapped mostly in the same well when the repulsive interspecies interaction strength grows larger than a critical value. After this sudden change, by further increasing u_{ab} up to 0.186 [Fig. 6(f)], the usual MS will be reached, with the phase-space domains of each species covering the same acreage in phase space.

As the strength of attractive interspecies interactions increases, we find that there exists nonlocal MS transition. The evolution scenario is shown in Fig. 7. Interestingly, we note that this scenario has many features in common with the scenario shown in Figs. 4(a)–(f). One major difference is the structure of the phase-space domains; one structure goes from top to bottom, whereas the other structure is embedded. This result can be understood by analyzing Eqs. (5)–(8). If we set S_a and S_b to have opposite signs and let u_{ab} also have a value with an opposite sign, the coupling term H_I does not change and neither H_a nor H_b changes. The two different initial conditions with opposite signs for the interspecies interactions correspond to the same Hamiltonian and consequently have the same dynamic evolution. This argument is also valid for the case of repulsive interspecies interaction in nonlocal π-phase mode in correspondence with Fig. 5.

Summarizing the above results, by increasing repulsive interspecies interactions, besides MS transitions, we find another counter-intuitive dynamical phase transition behavior: the merging of two separate phase domains with increasing repulsive interaction. By increasing attractive interspecies interactions, however, only one dynamical phase transition occurs, the nonlocalized MS transition.

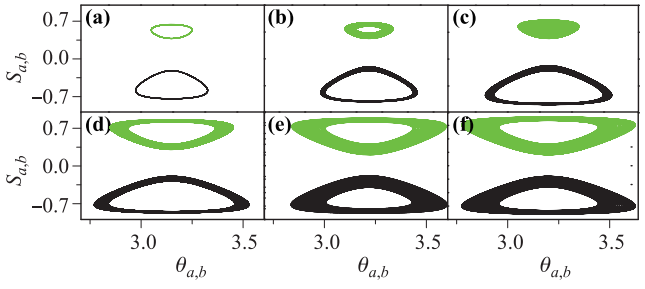

Fig. 7 Phase-space domains of the two species in the nonlocalized π-phase mode for $u_{ab} < 0$. The two species are represented by green and black. Initial configuration (S_a, S_b, θ_a, θ_b) set to be (-0.2, 0.4, π, π). **(a)** $u_{ab} = 0$. **(b)** $u_{ab} = -0.03$. **(c)** $u_{ab} = -0.0737$. **(d)** $u_{ab} = -0.1621$. **(e)** $u_{ab} = -0.1622$; Nonlocal MS is achieved. **(f)** $u_{ab} = -0.3$.

5 Bifurcations in 0 and π phase mode

In this section, we explore the mechanism of dynamical phase transitions in a two-species BJJ. Since we have learned that separatrix crossing is the dynamical mechanism behind various MS transitions [26], we will be concentrating on dynamical phase transitions other than MS transitions. Figures 8(a) and (b) show the bifurcation scenarios of the 0 phase mode for repulsive and attractive interspecies interactions, respectively. Further, Figs. 8(c) and (d) show the bifurcation scenarios for the π phase mode for repulsive and attractive interspecies interactions, respectively.

Figure 8(a) shows the bifurcation diagram for 0-phase modes with repulsive interspecies interactions. Overall, we see that by increasing u_{ab}, the red dotted-line transforms into black dotted-line, and there appear two more red dotted-curves. The red dots mark the stable fixed points, while the black dots mark the unstable fixed points. With $0 \leq u_{ab} < 2.2$, there is one stable fixed point "I"; at $u_{ab} = 2.2$, one reaches the bifurcation point. With $u_{ab} > 2.2$, two more "An" fixed points emerge. This is a typical supercritical pitchfork bifurcation scenario. A stable fixed point bifurcates into two new stable fixed points while the original becomes unstable. This naturally explains why there will be a dynamical phase transition of Josephson oscillation to self-trapped states.

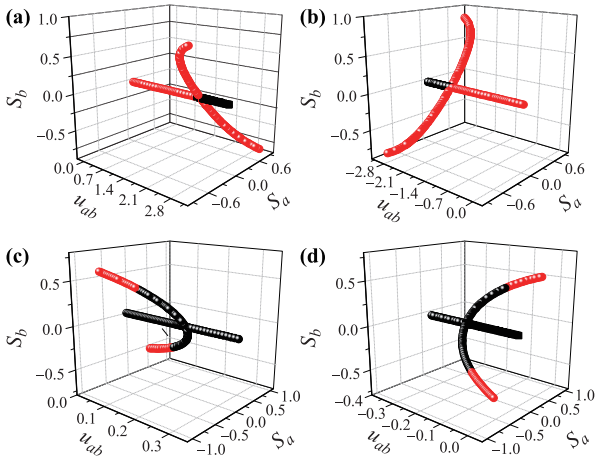

Fig. 8 The fixed point three-dimensional bifurcation diagram for 0-phase mode: **(a)** $u_{ab} > 0$, **(b)** $u_{ab} < 0$, and for π-phase mode: **(c)** $u_{ab} > 0$, **(d)** $u_{ab} < 0$.

Figure 8(b) shows that supercritical pitchfork bifurcation also occurs for the case of attractive interspecies interactions. With $-2.2 \leq u_{ab} < 0$, there is one stable fixed point "I"; at $u_{ab} = -2.2$, one reaches the bifurcation point. With $u_{ab} < -2.2$, there are two "S" fixed points that emerge beside the original "I" fixed point. Overall, one observes that the red dotted-line (stable) transforms into black dotted-line (unstable), and there appear two more red dotted-curves (stable). In another word, one stable "I" fixed point transforms into one unstable "I" fixed point with the appearance of two new stable "S" fixed points.

The bifurcation diagram for the π-phase modes are much more complicated, albeit we can have a simplified bifurcation diagram as shown in lower panel of Fig. 8, with Fig. 8(c) for repulsive interspecies interaction, and Fig. 8(d) for attractive interspecies interaction.

For repulsive interspecies interactions ($u_{ab} > 0$), starting with $u_{ab} = 0$, the "An" fixed points are stable, while the "I" fixed point is unstable. That is the reason why we can also have *nonlocal* π phase mode in the first place. For $u_{ab} > 0$, we notice that "An" fixed points are not always stable with increasing u_{ab}. It becomes unstable with $u_{ab} > 0.106728$. This instability leads to the breakdown of nonlocal MS states. As a result, chaos emerges as shown in Fig. 6(d). In addition, the "S" fixed points are the only fixed points that are stable with $u_{ab} > 0.106\,728$ [see Fig. 1(b)], so we end up with the localized π phase mode with u_{ab} continually increasing, as shown in Fig. 6(e).

For π-phase modes with increasing attractive interspecies interactions ($u_{ab} < 0$), we are in a similar situation as described above. For $u_{ab} = 0$, the "S" fixed points are stable along with stable "An" fixed points, while the "I" fixed point is unstable. Thus we can also have *localized* π phase mode with $u_{ab} = 0$ [Fig. 5(a)]. However, we notice that "S" fixed points are not always stable with $u_{ab} < 0$. On the other hand, the "An" fixed points are always stable with $u_{ab} < 0$, and "S" fixed points will become unstable with $u_{ab} < -0.106\,728$. This instability leads to the breakdown of the initial localized MS states. As a result, chaos emerges as shown in Fig. 5(d). In addition, the "An" fixed points will become the only stable points with $u_{ab} < -0.106\,728$ [see Fig. 1(e)]. Thus, we end up with the nonlocal π phase mode, as shown in Fig. 5(e).

6 Conclusion

To summarize, dynamical phase transitions in a two-species BJJ have been systematically studied. In the 0-phase mode, similar to the single-species BJJ system, we find that the two-species BJJ system also experiences dynamical phase transition from Josephson oscillation to self-trapping, which is induced by the enhanced nonlinear interaction $|u_{ab}|$. We further calculate the dynamical transition point for self-trapping, and find that the transition point is determined by the intrinsic parameters of the system and is fully independent of the exact initial conditions of the corresponding phase mode. This is different compared with the single-species BJJ case, for which it depends on the initial conditions [18].

Furthermore, in π-phase mode, we find two very counter-intuitive dynamical phase transitions. In the localized π-phase mode, we have characterized a phase separation behavior induced by increasing attractive interspecies interactions. On the contrary, in the nonlocal π-phase mode, a merging of two well-separated phase-space domains induced by increasing repulsive interspecies interaction has been characterized.

Finally, we reveal the mechanism behind all these dynamical phase transitions we have found. It is shown that various bifurcations scenarios can naturally explain the occurrence of these intriguing dynamical phase transitions.

With the experimental realization of bosonic Josephson junctions, it is expected that the intriguing phenomena we have characterized in phase space will be found in near future. A simple verification can be made by measuring the population imbalance for the two different species, and by focusing on the S axis of the phase space, we can get a glimpse of the phase space dynamics, i.e., the phase separation behavior in localized π-phase mode corresponds to an almost sudden sign change in population imbalance for one of the species. In addition, the interspecies interactions can be tuned by employing the Feshbash resonance technique. These are well within the reach of experiment toolboxes.

Acknowledgements This work was supported by the National Natural Science Foundation of China (Grant Nos. 11104217 and 11402199), the Science Plan Foundation office of the Education Department of Shaanxi Province (Grant No. 14JK1676), and the Natural Science Foundation of Shaanxi Province (Grant No. 14JQ1022).

References

1. V. M. Pérez-García, N. G. Berloff, P. G. Kevrekidis, V. V. Konotop, and B. A. Malomed, Nonlinear phenomena in degenerate quantum gases, *Physica D* 238(15), 1289 (2009)
2. O. Morsch and M. Oberthaler, Dynamics of Bose–Einstein condensates in optical lattices, *Rev. Mod. Phys.* 78(1), 179 (2006)
3. C. J. Pethick and H. Smith, Bose–Einstein Condensation in Dilute Gases, Cambridge: Cambridge University

Press, 2008

4. H. L. Zheng and Q. Gu, Dynamics of Bose–Einstein condensates in a one-dimensional optical lattice with double well potential, *Front. Phys.* 8(4), 375 (2013)
5. X. F. Zhang, X. H. Hu, D. S. Wang, X. X. Liu, and W. M. Liu, Dynamics of Bose–Einstein condensates near Feshbach resonance in external potential, *Front. Phys.* 6(1), 46 (2011)
6. L. Khaykovich, F. Schreck, G. Ferrari, T. Bourdel, J. Cubizolles, L. D. Carr, Y. Castin, and C. Salomon, Formation of a matter-wave bright soliton, *Science* 296(5571), 1290 (2002)
7. K. W. Madison, F. Chevy, W. Wohlleben, and J. Dalibard, Vortex formation in a stirred Bose–Einstein condensate, *Phys. Rev. Lett.* 84(5), 806 (2000)
8. A. Smerzi, S. Fantoni, S. Giovanazzi, and S. R. Shenoy, Quantum coherent atomic tunneling between two trapped Bose–Einstein condensates, *Phys. Rev. Lett.* 79(25), 4950 (1997)
9. H. B. Qiu, J. Tian, and L. B. Fu, Collective dynamics of two-species Bose–Einstein-condensate mixtures in a double-well potential, *Phys. Rev. A* 81(4), 043613 (2010)
10. T. Zibold, E. Nicklas, C. Gross, and M. K. Oberthaler, Classical bifurcation at the transition from Rabi to Josephson dynamics, *Phys. Rev. Lett.* 105(20), 204101 (2010)
11. H. Hennig, D. Witthaut, and D. K. Campbell, Global phase space of coherence and entanglement in a double well Bose–Einstein condensate, *Phys. Rev. A* 86(5), 051604 (2012)
12. G. J. Krahn and D. H. J. O'Dell, Classical versus quantum dynamics of the atomic Josephson junction, *J. Phys. At. Mol. Opt. Phys.* 42(20), 205501 (2009)
13. M. Chuchem, K. Smith-Mannschott, M. Hiller, T. Kottos, A. Vardi, and D. Cohen, Quantum dynamics in the bosonic Josephson junction, *Phys. Rev. A* 82(5), 053617 (2010)
14. K. Sakmann, A. I. Streltsov, O. E. Alon, and L. S. Cederbaum, Exact quantum dynamics of a bosonic Josephson junction, *Phys. Rev. Lett.* 103(22), 220601 (2009)
15. R. Hipolito and A. Polkovnikov, Breakdown of macroscopic quantum self-trapping in coupled mesoscopic one dimensional Bose gases, *Phys. Rev. A* 81(1), 013621 (2010)
16. B. Juliá-Díaz, D. Dagnino, M. Lewenstein, J. Martorell, and A. Polls, Macroscopic self-trapping in Bose–Einstein condensates: Analysis of a dynamical quantum phase transition, *Phys. Rev. A* 81(2), 023615 (2010)
17. S. Levy, E. Lahoud, I. Shomroni, and J. Steinhauer, The ac and dc Josephson effects in a Bose–Einstein condensate, *Nature* 449(7162), 579 (2007)
18. L. B. Fu and J. Liu, Quantum entanglement manifestation of transition to nonlinear self-trapping for Bose–Einstein condensates in a symmetric double well, *Phys. Rev. A* 74(6), 063614 (2006)
19. S. Ashhab and C. Lobo, External Josephson effect in Bose–Einstein condensates with a spin degree of freedom, *Phys. Rev. A* 66(1), 013609 (2002)
20. B. Sun and M. S. Pindzola, Dynamics of a two-species Bose–Einstein condensate in a double well, *Phys. Rev. A* 80(3), 033616 (2009)
21. B. Juliá-Díaz, M. Guilleumas, M. Lewenstein, A. Polls, and A. Sanpera, Josephson oscillations in binary mixtures of $F = 1$ spinor Bose–Einstein condensates, *Phys. Rev. A* 80(2), 023616 (2009)
22. A. Naddeo and R. Citro, Quantum Bose–Josephson junction with binary mixtures of BECs, *J. Phys. At. Mol. Opt. Phys.* 43(13), 135302 (2010)
23. S. K. Adhikari, Self-trapping of a binary Bose–Einstein condensate induced by interspecies interaction, *J. Phys. At. Mol. Opt. Phys.* 44(7), 075301 (2011)
24. I. I. Satija, R. Balakrishnan, P. Naudus, J. Heward, M. Edwards, and C. W. Clark, Symmetry-breaking and symmetry-restoring dynamics of a mixture of Bose–Einstein condensates in a double well, *Phys. Rev. A* 79(3), 033616 (2009)
25. G. Mazzarella, B. Malomed, L. Salasnich, M. Salerno, and F. Toigo, Rabi-Josephson oscillations and self-trapped dynamics in atomic junctions with two bosonic species, *J. Phys. At. Mol. Opt. Phys.* 44(3), 035301 (2011)
26. J. Tian, H. B. Qiu, G. F. Wang, Y. Chen, and L. B. Fu, Measure synchronization in a two-species bosonic Josephson junction, *Phys. Rev. E* 88(3), 032906 (2013)
27. S. Raghavan, A. Smerzi, S. Fantoni, and S. R. Shenoy, Coherent oscillations between two weakly coupled Bose–Einstein condensates: Josephson effects, π oscillations, and macroscopic quantum self-trapping, *Phys. Rev. A* 59(1), 620 (1999)
28. A. J. Leggett, Bose–Einstein condensation in the alkali gases: Some fundamental concepts, *Rev. Mod. Phys.* 73(2), 307 (2001)
29. S. B. Papp and C. E. Wieman, Observation of heteronuclear Feshbach molecules from a $Rb^{85}Rb^{87}$ gas, *Phys. Rev. Lett.* 97(18), 180404 (2006)
30. A. Hampton and D. H. Zanette, Measure synchronization in coupled Hamiltonian systems, *Phys. Rev. Lett.* 83(11), 2179 (1999)
31. J. Tian, H. B. Qiu, and Y. Chen, Nonlocal measure synchronization in coupled bosonic Josephson junctions, *Chin. Phys. Lett.* 27(7), 070501 (2010)